JOURNAL OF THERMOPHYSICS AND HEAT TRANSFER
Vol. 23, No. 4, October–December 2009

Technical Notes

Heat Transfer Phenomena in a Vortex Engine

M. Kargar,* M. H. Saidi,† and A. Ghafourian‡
Sharif University of Technology, 11115-9567 Tehran, Iran

DOI: 10.2514/1.37278

Nomenclature

A	=	heat transfer area, m^2
b	=	nozzle radius, m
c_p	=	specific thermal capacity, $J/kg \cdot K$
D	=	outer diameter of chamber, m
e_r	=	radial unit vector component
e_z	=	axial unit vector component
e_θ	=	tangential unit vector component
F	=	fuel mass flow rate, kg/s
h	=	height of steal segments, m
k	=	conductivity, $W/m \cdot K$
L	=	length of chamber, m
mo	=	oxidizer (air + pure O2) mass flow rate, kg/s
p	=	static pressure, Pa
Q	=	volumetric flow rate, m^3/s
$\dot{Q}$	=	rate of heat transfer, W
q''	=	heat flux, W/m^2
R	=	inner radius of chamber, m
r	=	radial coordinate
T	=	temperature, K
t	=	time, s
U	=	velocity of tangentially injected oxidizer, m/s
u_z	=	axial velocity, m/s
z	=	axial coordinate
ρ	=	density, kg/m^3

Subscripts

a	=	actual
C	=	convective cooling
f	=	fuel
in	=	inner side
o	=	oxidizer
out	=	outer side
r	=	radial coordinate
R	=	radiation heat transfer
s	=	stoichiometric
T	=	total heat transfer
z	=	axial coordinate
θ	=	tangential coordinate

Presented as Paper 5586 at the 43rd AIAA/ASME/SAE/ASEE Joint Propulsion Conference and Exhibit, Cincinnati, OH, 8–11 July 2007; received 24 February 2008; revision received 12 March 2009; accepted for publication 10 May 2009.

*M.Sc. Graduate, Center of Excellence in Energy Conversion, School of Mechanical Engineering. Student Member AIAA.
†Professor, Center of Excellence in Energy Conversion, School of Mechanical Engineering.
‡Assistant Professor, Department of Aerospace Engineering.

I. Introduction

CYCLONIC flows are characterized by a bidirectional coaxial swirl motion that is not caused by vortex breakdown or instability. Because of the flow reversal in the conical section of a cyclone, the primary flow is forced to turn around as the core is approached. Many researchers have worked on the hydrodynamics of cyclonic flows. The theory beyond cyclonic flows was modeled basically by Bloor and Ingham [1]. They used a simple analytical method to derive the governing relation of tangential velocity in a cyclone. Neglecting viscosity, they developed a complementary analytic solution to fluid dynamic problem of cyclones [2], by assuming a power law to find streamlines. Having the assumptions of steady, axisymmetric, incompressible and inviscid flow, they found fairly good relations which are still in use.

Cyclone combustion chambers have been developed in many forms, but they have usually been used for the combustion and processing of materials that are normally considered difficult to burn or process efficiently such as vegetable refuse, high ash content coals, anthracite, high sulfur oils, low calorific value waste gas, certain mineral ores, and as part of magnetohydrodynamic combustors [3]. Recently cyclonic flows are used to achieve lower wall temperature rather than axial common burners. In this method (Fig. 1), oxidizer issues tangentially at the partially open end of the chamber and consequently, a cool vortex flows toward the closed head, being mixed with fuel. A secondary vortex of combustible reactants swirls coaxial with the first vortex to the nozzle exit. The first prototype engine is due to the work of Chiaverini et al. [4], called the cold-wall bidirectional vortex combustion chamber. In this chamber a full reverse bidirectional swirl flow is implemented. Vyas et al. [5,6] worked on the fluid dynamic problem of the bidirectional swirl combustor analytically. Having used the assumptions of steady, incompressible, inviscid and axisymmetric, they found a complete formulation of velocity field and pressure distribution along all directions of the cylindrical coordinate. Their solution deteriorates near the centerline due to the inviscid flow assumption; therefore they modified the obtained solution by extending the viscosity effects in the interior core region [7].

Chiaverini et al. [8] developed some experiments on two types of vortex combustion cold-wall thrust chambers to determine the effects of the combustion chamber, nozzle geometry, and injection parameters on specific impulse performance and chamber thermal behavior. They used semi-empirical correlations to estimate the relative magnitude of thermal radiation and convection on the chamber sidewalls and finally concluded that chamber sidewall heating rates did not display a significant dependence on chamber pressure, apparently due to the similar effects of elevated pressure on both

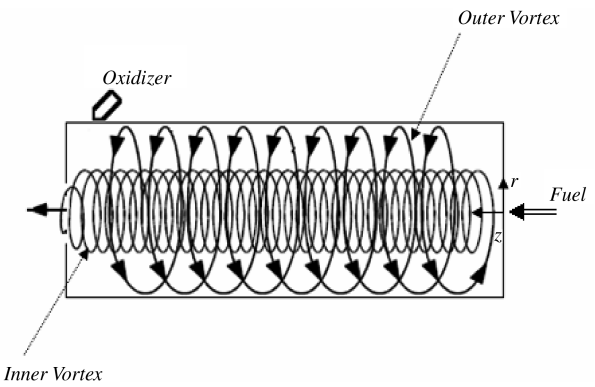

Fig. 1 Bidirectional swirl flow in a cylinder.

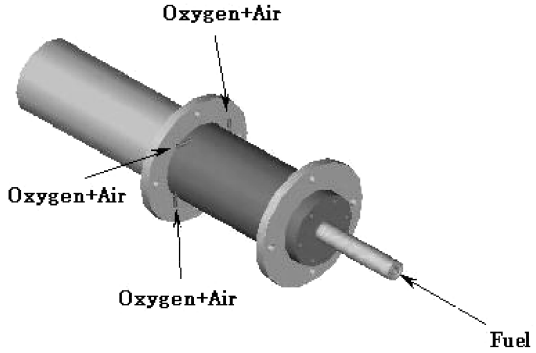

Fig. 2 Fuel enters to the chamber head and air plus oxygen enter tangentially to the chamber base.

thermal radiation and convective cooling from the outer vortex. Ghafourian et al. [9] performed an experimental research on a bidirectional swirl chamber, namely, the vortex engine. They found that the highly convective coolant flow of outer vortex reduces the temperature about 70% alleviation in the sidewall temperature, compared with the usual combustion chamber with oxygen and fuel both issuing from the top. This research will focus on the investigation of the heat transfer phenomena in a vortex engine.

II. Vortex Engine Theories

Figure 1 shows the typical geometry of the vortex engine. In this geometry a close head and partially open end are assumed. By ignoring the small transition zone at the inlet to the chamber, the rest of the flow is axisymmetric; by assuming a steady, inviscid, incompressible, rotational, and nonreacting flow, the axial and radial velocities and their concerned pressure gradients have been obtained by Vyas et al. [5,6]:

$$u = -\frac{Q\sin(\pi r^2/R^2)}{2\pi Lr}e_r + \frac{UR}{r}e_\theta + \frac{Qz\cos(\pi r^2/R^2)}{LR^2}e_z$$

$$\frac{\partial p}{\partial z} = \frac{\rho Q^2}{R^4L^2} \tag{1}$$

u_z shows the existence of a bidirectional swirl flow. A cold oxidizer injected tangentially from the open end will swirl upward on the vicinity of the wall. u_r shows a radial flow from the outer vortex to the inner one, so the oxidizer mixes with fuel in the core and swirls down the chamber through a core flow. This means that in the ideal case, the reaction will occur completely in the core and a cold flow of oxidizer flows near the wall. Experiments of Saidi et al. [10] show that assuming ideal conditions are a good approximation and therefore convective cooling can be estimated as the difference between radiation and total heat transfers as noted in the following equation:

$$\dot{Q}_C = \dot{Q}_R - \dot{Q}_T \tag{2}$$

III. Experiments

A. Description of Test Rig

The combustion chamber includes a fuel inlet flow pipe at the chamber head, four tangential inlet pipes at the chamber end, exhaust

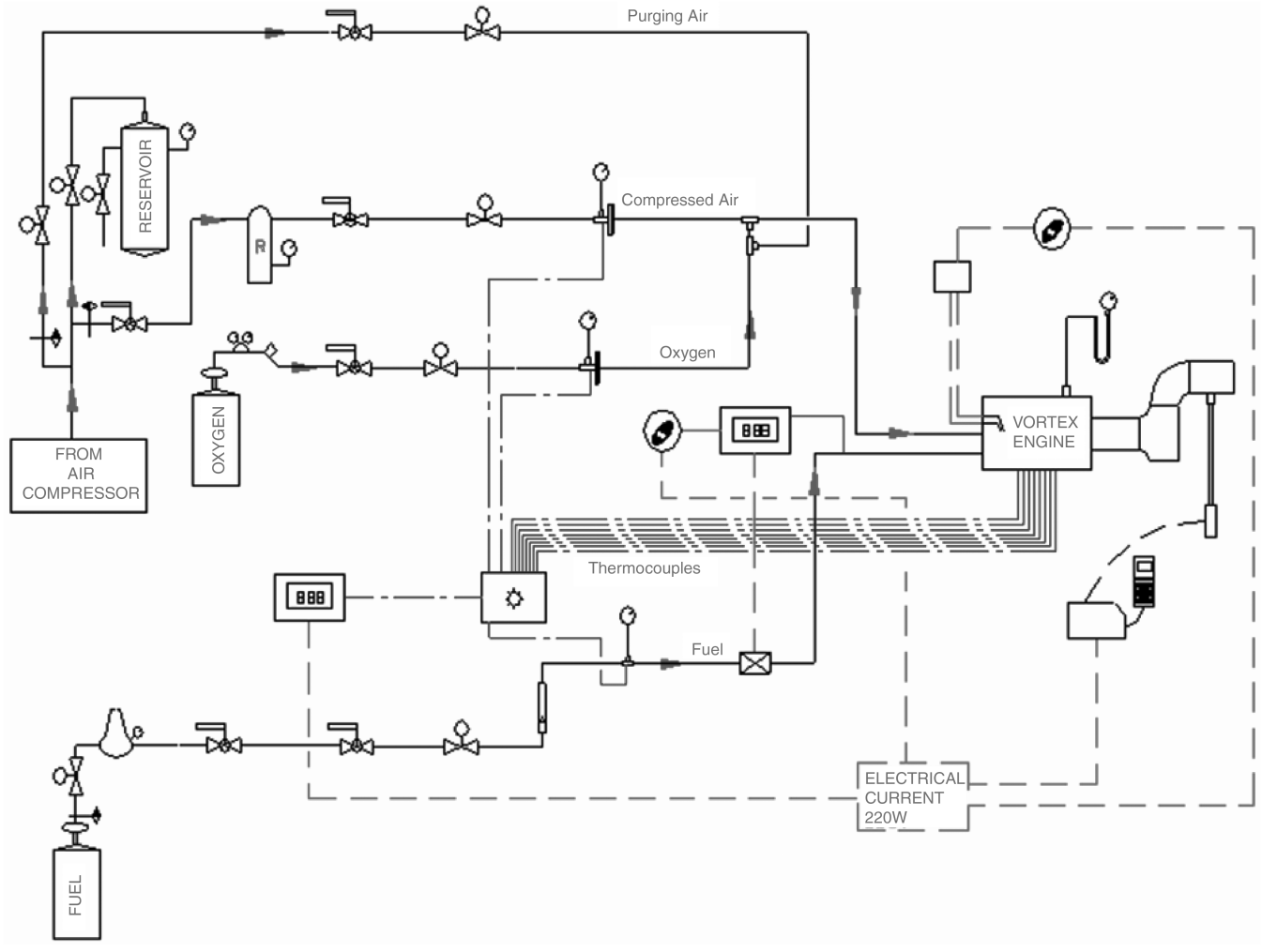

Fig. 3 Flow diagram and instrumentation of the test rig.

Table 1 Characteristics of the combustion chamber

Material	C40 steel
Inside diameter	154 mm
Thickness	20.4 mm
Lengths	250 mm
Exhaust nozzle diameter	108 mm

nozzle, and diagnostic ports. In all experiments, fuel enters from the head and the oxidizer enters tangentially from the base as shown in Fig. 2.

The oxidizer feeding system supplies the required oxidizer to the chamber. Air enriched with oxygen is used as the oxidizer. A fuel feeding system supplies the fuel to the chamber. A mixture of butane and propane is used as the fuel in which the mole fraction of butane and propane is 0.2 and 0.8, respectively. Figure 3 shows the flow diagram and instrumentation of the test rig. In experiments, the equivalence ratio (ER) is defined as

$$\mathrm{ER} = \frac{(F/\text{oxidizer})_a}{(F/\text{oxidizer})_s} \tag{3}$$

In this definition the oxygen content of air plus pure injected oxygen is considered as an oxidizer, but in other cases the oxidizer mass flow rate is defined as the total mass flow rate of air plus the mass flow rate of pure oxygen. Table 1 shows the properties of the thick wall chamber used in the experiments.

B. Measurement Systems

To measure heat transfer, four square-shaped holes have been created in the chamber wall shown in Fig. 4. Four segments from ST 38 steel with a thermocouple of *K* type in each side fill up the wholes. There is an air gap between segments and holes which is filled up with ceramic blanket insulation to protect segments from direct contact with the chamber wall; therefore, the axial conduction is negligible. To measure the rate of total heat transfer, all segments must be in direct contact with combustion gases. In this case the lower face of segments curved, based on the curvature of the chamber wall to minimize perturbation on the flowfield. In the other series of experiments, the segments are protected from direct contact with hot combustion gases using a quartz window. Finding the rates of total and radiation heat transfer, convective cooling can be calculated using Eq. (3).

Sonic nozzles are used to meter the mean mass flow rates of air and oxygen lines and a calibrated Rotameter is used to measure fuel flow rate. All thermocouples are connected to a selector and the selector is connected to a digital indicator which sows selected temperature with a tolerance of ±0.5°C.

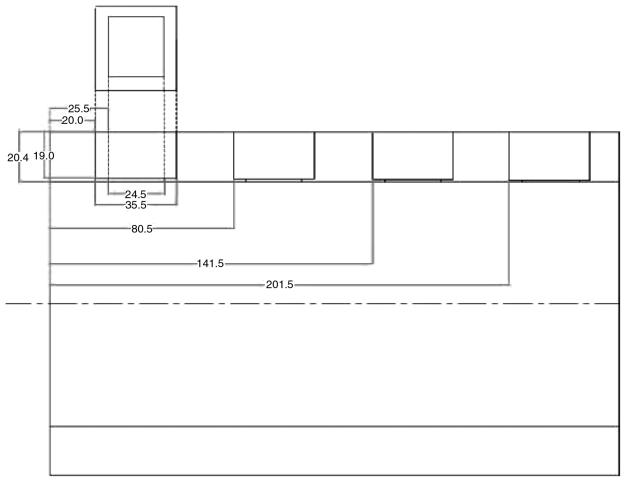

Fig. 4 Configuration of the holes in the chamber wall (dimensions in millimeters).

C. Tests Procedure

A series of tests has been conducted in different conditions of oxidizer and fuel mass flow rates for a vortex engine. The time of the tests is kept short enough in such a way that the conditions remain constant for all measuring points, but when the variation in the combustor operating conditions is observed, the test is repeated. The tests are categorized into two groups to find 1) the effects of the oxidizer mass flow rate on the flux of radiation heat transfer and convective cooling at a fixed equivalence ratio, and 2) the effects of the equivalence ratio on the considering heat transfer phenomena at a fixed oxidizer mass flow rate. For the first group, the mole fraction of nitrogen in the oxidizer is kept approximately constant and equal to 0.64 ± 0.007, but for the other group of tests the mole fraction of nitrogen in the oxidizer kept exactly constant and equal to 0.639. To calculate the rate of heat transfer to the chamber wall by Eq. (4), the heat transfer in the chamber wall must reach a steady-state condition. In all experiments the steady-state conditions are defined as follows:

$$\frac{\partial T}{\partial t} < 1 \frac{^\circ\mathrm{C}}{\mathrm{min}} \tag{4}$$

Using this condition the average required time to reach the steady-state condition is equal to 62 min. Figure 5 shows the steady-state temperature distribution of the inner and outer sides of the chamber for ER = 1.02 and $mo = 2.842$ g/s.

D. Uncertainties

Using the Fourier law, the heat fluxes reaching the segments can be estimated by the following equation:

$$q'' = \dot{Q}/A = k\frac{T_{\mathrm{in}} - T_{\mathrm{out}}}{h} \tag{5}$$

Based on Eq. (4), the uncertainties on the measured heat fluxes can be calculated as

$$\frac{\delta q''}{q''} = \frac{\delta k}{k} + \frac{\delta(\Delta T)}{\Delta T} + \frac{\delta h}{h} \tag{6}$$

in which we have $\Delta T = T_{\mathrm{in}} - T_{\mathrm{out}}$, $\delta(\Delta T) = 1^\circ\mathrm{C}$, $h = 20.4$ mm, and $\delta h = 0.01$ mm. In the temperature range of the experiments the thermal conductivity of ST 38 steel has a near-linear relation with the temperature, so in the range of the steady temperatures of experiments the first term $\delta k/k$ is negligible in comparison with the second term. The last term, $\delta h/h$, is approximately equal to 0.0005. So the uncertainties can be predicted with Eq. (7):

$$\frac{\delta q''}{q''} \approx \frac{\delta(\Delta T)}{\Delta T} \tag{7}$$

Based on Eq. (2), the uncertainty of convective cooling has been calculated by Eq. (8):

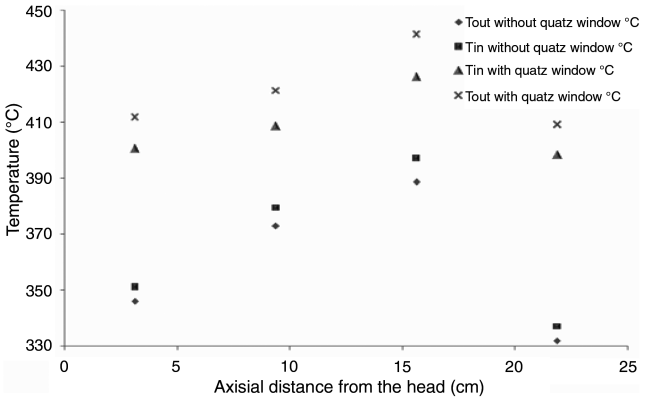

Fig. 5 Steady temperature distribution of the chamber wall (ER = 1.02 and *mo* = 2.842).

Table 2 Uncertainty distribution for different oxidizer mass flow rates, %

Axial position, cm	Oxidizer mass flow rate, g/s				
Total	3.438	3.162	2.842	2.614	2.246
21.8	—	—	—	—	—
15.6	14	13	12	10	10
9.3	20	17	15	13	12
3.1	29	22	20	17	15
Radiation					
21.8	9	9	9	9	9
15.6	7	7	7	6	6
9.3	8	8	8	7	7
3.1	9	9	9	8	8
Convection					
21.8	—	—	—	—	—
15.6	21	19	18	16	15
9.3	28	25	23	21	19
3.1	—	—	29	25	23

Table 3 Uncertainty distribution for different equivalence ratios, %

Axial position, c	Equivalence ratio				
Total	0.81	0.92	1.02	1.12	1.22
21.8	—	—	—	—	—
15.6	14	13	12	12	12
9.3	20	18	15	15	13
3.1	25	22	20	18	17
Radiation					
21.8	10	10	9	9	9
15.6	7	7	7	7	7
9.3	8	8	8	8	8
3.1	10	10	10	9	9
Convection					
21.8	—	—	—	—	—
15.6	21	19	18	18	18
9.3	28	26	23	23	21
3.1	—	—	—	27	26

$$\frac{\delta q''_C}{q''_C} = \frac{\delta q''_R}{q''_R} + \frac{\delta q''_T}{q''_T} \tag{8}$$

Neglecting results with an uncertainty of more than 30%, Tables 2 and 3 show the uncertainty distribution along the chamber for the equivalence ratio equal to 1.02 and oxidizer mass flow rate equal to 2.842 g/s, respectively.

IV. Results and Discussion

The radiation heat flux for the corresponding equivalence ratio of 1.02 and oxidizer mass flow rate of 2.842 g/s have been shown in Figs. 6 and 7, respectively.

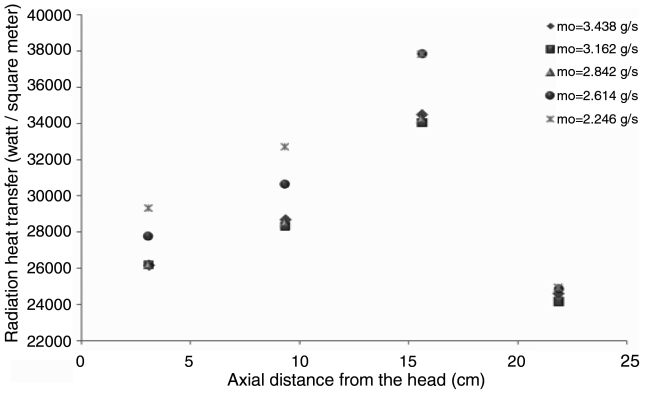

Fig. 6 The rate of radiation heat transfer to the chamber wall (ER = 1.02).

Figures 6 and 7 show that the rate of radiation heat transfer to the chamber wall primarily increases by increasing the axial distance from the closed head; however, at the final section of the chamber, it descends. Considering the results of [10], for the local heat release and equivalence ratio distribution in the same range we know that in the middle sections of the chamber the reaction is stronger than the other parts. At the initial sections of the chamber, the rate of reaction is low and as the flow passes through the chamber the rate of mixing increases, but at the end of the chamber the rate of reaction decreases. Figure 8 shows the distribution of C_2^* chemiluminescence emissions as a representative of the equivalence ratio along the chamber centerline for both a common axial-type burner and a vortex engine in the same condition [11].

As Figs. 9 and 10 show, convective cooling is approximately an increasing function of the axial distance from the closed head. The oxidizer is entered tangentially to the chamber at the open end with temperature equal to 21°C. But as it moves toward the chamber's closed end the oxidizer mass flow rate at axial and tangential directions decreases due to the radial flow of the oxidizer from the outer to the inner vortex. On the other hand, the heat transfer from the flame and the chamber wall to the cold oxidizer flow will increase its temperature and the rate of temperature rising will be different depending on the distribution of the heat release rate. It is important to note that passing thorough the chamber cooling flow will encounter other recirculation zones in a cyclonic flow like a longitudinal recirculation zone between the inner and the outer vortex [3], which will affect its temperature and composition. Figures 9 and 6, respectively, show approximately a direct relation between convective cooling flux and oxidizer mass flow rate and a reverse relation between radiation heat flux and oxidizer mass flow rate. Also this effect diminishes at the higher oxidizer flows. From the results of Figs. 8 and 10, it can be seen that the increasing equivalence ratio at a fixed oxidizer mass flow rate, approximately, has a direct effect on the

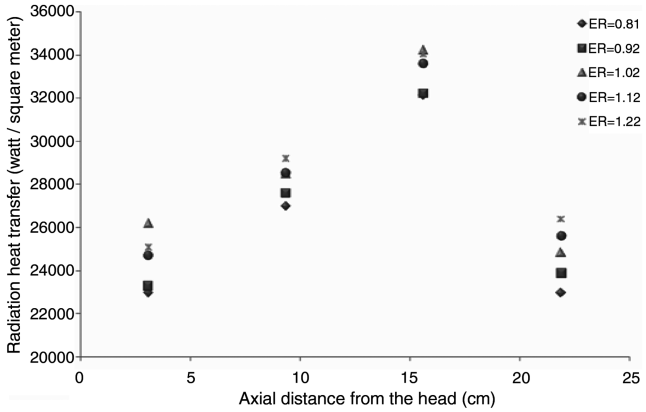

Fig. 7 The rate of radiation heat transfer to the chamber wall (*mo* = 2.842 g/s).

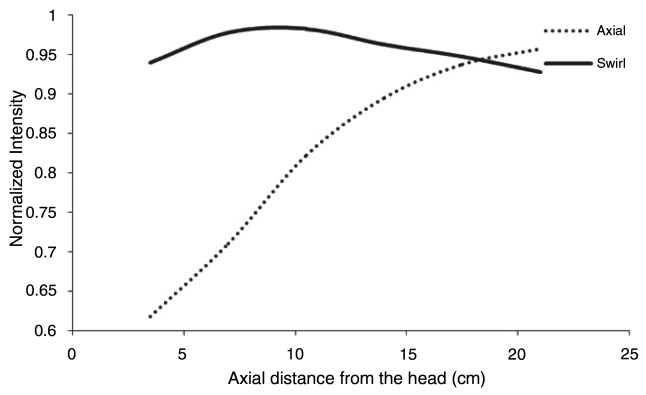

Fig. 8 Normalized intensity of C_2^* emissions along the chamber axis (ER = 1.02 and *mo* = 2.842 g/s) [11].

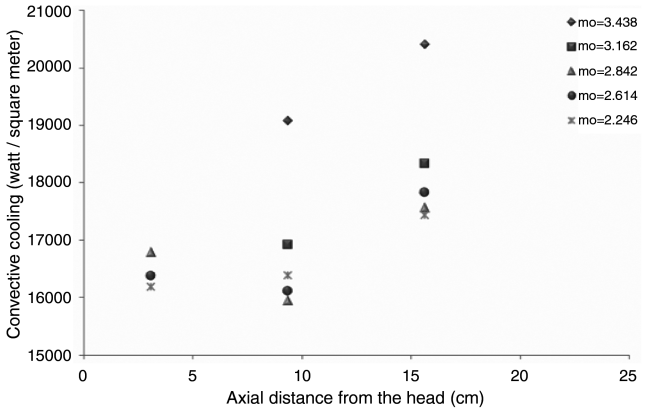

Fig. 9 The rate of convective cooling performed with the outer vortex (ER = 1.02).

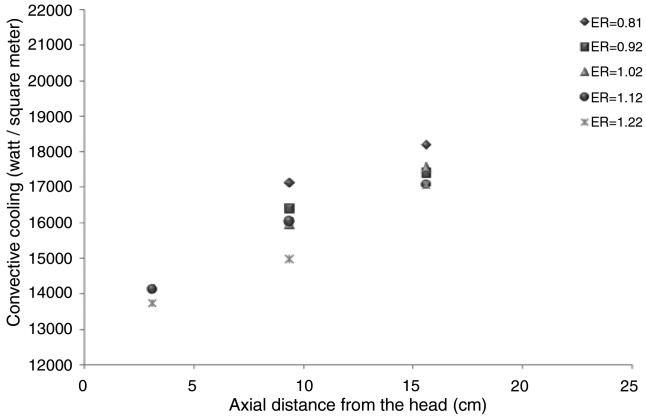

Fig. 10 The rate of convective cooling performed with the outer vortex ($mo = 2.842$ g/s).

radiation heat transfer to the chamber wall. As shown in Fig. 10, the effect of the equivalence ratio at a fixed oxidizer mass flow rate on convective cooling is different along the chamber length, but it is approximately an inverse relation between the cooling rate and the equivalence ratio. Increasing the equivalence ratio at a fixed oxidizer mass flow rate is equivalent to the increase of the fuel mass flow rate at a fixed oxidizer mass flow rate. At a fixed oxidizer mass flow rate, the conditions of a newly arrived cooling oxidizer to the chamber is the same for all equivalence ratios, but by moving toward the closed head, the different rate of heat release from the flame affects the conditions of the cooling media.

V. Conclusions

The rates of total and radiative heat transfers are measured experimentally, and the convective cooling is calculated from the difference between the two above mentioned quantities. It was observed that the radiation heat transfer is the dominant mode of heat transfer in a vortex engine which causes a rise in the temperature of the chamber wall; however, convective cooling provided by an outer cooled vortex decreases the wall temperature. The average convective cooling rate is around 62% of the radiation heat transfer. The effects of the oxidizer mass flow rate and the equivalence ratio on the heat transfer mode are presented as well.

References

[1] Bloor, M. I. G., and Ingham, D. B., "Theoretical Investigation of the Flow in a Conical Hydrocyclone," *Transactions of the Institution of Chemical Engineers*, Vol. 51, 1973, pp. 36–41.

[2] Bloor, M. I. G., and Ingham, D. B., "The Flow in Industrial Cyclones," *Journal of Fluid Mechanics*, Vol. 178, 1987, pp. 507–519. doi:10.1017/S0022112087001344

[3] Gupta, A. K., Lilley, D. G., and Syred, N., *Swirl Flows*, Abacus Press, Tunbridge Wells, 1985.

[4] Chiaverini, M. J., Malecki, M. J., Sauer, J. A., and Knuth, W. H., "Vortex Combustion Chamber Development for Future Liquid Rocket Engine Applications," AIAA Paper 2002-2149, July 2002.

[5] Vyas, A. B., Majdalani, J., and Chiaverini, M. J., "The Bidirectional Vortex. Part 1: An Exact Inviscid Solution," AIAA Paper 2003-5052, 2003.

[6] Vyas, A. B., Majdalani, J., and Chiaverini, M. J., "Exact Solution of the Bidirectional Vortex," *AIAA Journal*, Vol. 44, No. 10, 2006, pp. 2208–2216. doi:10.2514/1.14872

[7] Vyas, A. B., Majdalani, J., and Chiaverini, M. J., "The Bidirectional Vortex. Part 2: Viscous Core Corrections," AIAA Paper 2003-5053, 2003.

[8] Chiaverini, M. J., Malecki, M. J., Sauer, A., Knuth, W. H., Gramer, D. J., and Majdalani, J., "Vortex Thrust Chamber Testing and Analysis for O2-H2 Propulsion Applications," AIAA 2003-4473, 2003.

[9] Ghafourian, A., Saidi, M. H., Jahangirian, S., and Abarham, M., "Effect of Vortex Flow on Heat Transfer to Combustion Chamber Wall," *Journal of Engineering for Gas Turbines and Power*, Vol. 129, No. 2, 2007, pp. 622–624. doi:10.1115/1.2431386

[10] Saidi, M. H., Ghafourian, A., Kargar, M., and Faisal, M., "Swirl Flow Effects on Heat Release/ Luminous Radiation from Flame in Vortex Engines," *ASME Joint, U.S.—European Fluids Engineering Summer Meeting FEDSM2006*, American Society of Mechanical Engineers, Fairfield, NJ, 2006.

[11] Kargar, M., "Experimental and Theoretical Investigation of Combustion Quality and Heat Radiation in a Vortex Engine," M.Sc. Thesis, Mechanical Engineering Department, Sharif University of Technology, Tehran, Iran, 2006.